NIH Public Access
Author Manuscript
*Optom Vis Sci*. Author manuscript; available in PMC 2009 July 23.

Published in final edited form as:
*Optom Vis Sci*. 2008 June ; 85(6): 425–435. doi:10.1097/OPX.0b013e31817841cb.

# The Mechanical Environment of the Optic Nerve Head in Glaucoma

**J. Crawford Downs, PhD**[1], **Michael D. Roberts, PhD**[1], and **Claude F. Burgoyne, MD**[2]

[1]Ocular Biomechanics Laboratory Devers Eye Institute Legacy Health System Portland, Oregon, USA

[2]Optic Nerve Head Research Laboratory Devers Eye Institute Legacy Health System Portland, Oregon, USA

## I. The Optic Nerve Head (ONH) as a Biomechanical Structure

The ONH is of particular interest from a biomechanical perspective because it is a weak spot within an otherwise strong corneo-scleral envelope. While there are likely to be important pathophysiologies within the retinal ganglion cell stroma, photoreceptors, lateral geniculate body and visual cortex[1-8] most evidence suggests that damage to the retinal ganglion cell axon within the lamina cribrosa is the principal pathophysiology underlying glaucomatous vision loss and optic nerve head cupping.[5-7].

The lamina cribrosa provides structural and functional support to the RGC axons as they pass from the relatively high-pressure environment in the eye to a low-pressure region in the retrobulbar cerebrospinal space. To protect the RGC axons within this unique environment, the lamina cribrosa in higher primates has developed into a complex structure composed of a three-dimensional (3D) network of flexible beams of connective tissue (Figure 1). The ONH is nourished by the short posterior ciliary arteries, which penetrate the immediate peripapillary sclera to feed capillaries contained within the laminar beams. This intra-scleral and intra-laminar vasculature is unique in that it is encased in load-bearing connective tissue, either within the scleral wall adjacent to the lamina cribrosa, or within the laminar beams themselves (Figure 1). Glaucoma is a multifactorial disease, and we believe that biomechanics not only determines the mechanical environment in the ONH, but also mediates IOP-related reductions in blood flow and cellular responses through various pathways (Figure 2).

Consideration of the anatomy of the lamina cribrosa and peripapillary sclera suggests that the classic “mechanical” and “vascular” mechanisms of glaucomatous injury are inseparably intertwined (Figures 1 and 2). For example, prior to structural damage, IOP-related stress could detrimentally affect the blood supply to the laminar segments of the axons through deformation of the capillary-containing laminar beams. Also, IOP-related remodeling of the extracellular matrix (ECM) of the laminar beams could limit the diffusion of nutrients to RGC axons in the ONH. Reciprocally, primary insufficiency in the blood supply to the laminar region could induce cell-mediated connective tissue changes that would serve to weaken the laminar beams, making them more prone to failure under previously “safe” levels of IOP-related mechanical stress.

To incorporate these concepts into a global conceptual framework, we have previously proposed that the ONH is a biomechanical structure[8]. This paradigm assumes that IOP-related stress (force/cross sectional area) and strain (local deformation of the tissues) are central

Correspondence: J. Crawford Downs, PhD Devers Eye Institute Ocular Biomechanics Laboratory 1225 NE 2nd Avenue Portland, Oregon, 97232, USA Phone: 503−413−5320 Fax: 503−413−5179 E-mail: cdowns@deverseye.org.

NIH-PA Author Manuscript
NIH-PA Author Manuscript
NIH-PA Author Manuscript

NIH-PA Author Manuscript

NIH-PA Author Manuscript

NIH-PA Author Manuscript

determinants of both the physiology and pathophysiology of the ONH tissues and their blood supply (Figure 2) at all levels of IOP. These changes include not only alterations to the load-bearing connective tissues of the lamina cribrosa and the peripapillary sclera, but also the cellular components of these tissues (astrocytes, glia, endothelial cells, and pericytes, along with their basement membranes) and the RGC axons in the ONH. Experienced over a lifetime at physiologic levels, they underlie “normal” ONH aging. However, acute or chronic exposure to pathophysiologic levels results in glaucomatous damage.

Although IOP-lowering remains the only proven method of preventing the onset and progression of glaucomatous vision loss, the role of IOP in the development and progression of the neuropathy remains controversial. This largely arises from the clinical observation that significant numbers of patients with statistically normal levels of IOPs develop glaucoma (*e.g*. normotensive glaucoma), while other individuals with elevated IOP may show no signs of the disease over extended periods of observation.

While there is a wide spectrum of individual susceptibility to IOP-related glaucomatous vision loss, the biomechanical effects of IOP on the tissues of the optic nerve head likely play a central role in the development and progression of the disease at all IOPs. Our paradigm suggests that the susceptibility of a particular patient's ONH to IOP insult is likely a function of the biomechanical response of the constituent tissues and the resulting mechanical, ischemic and cellular events driven by that response. Hence eyes with a particular combination of connective tissue geometry, stiffness and blood supply may be more susceptible to damage at normal levels of IOP, while others may have a combination of these central susceptibility variables that can withstand prolonged periods of relatively high levels of IOP.

## II. Mechanical Environment of the Optic Nerve Head and Peripapillary Sclera

### A. Basic Engineering Concepts

The following are fundamental terms and concepts from engineering mechanics that may not be familiar to clinicians and non-engineering scientists. The interested reader may pursue these ideas in greater depth by referring to appropriate textbooks on engineering science, mechanics of materials, and biomechanics[9, 10].

***Stress*** is a measure of the load applied to, transmitted through, or carried by a material or tissue. Stress can be defined as the amount of force applied to a tissue divided by the cross sectional area over which it acts (e.g. pressure is a stress and can be expressed in pounds per square inch (psi)). Because tissues generally exhibit spatial variations in shape and cross sectional area and the points of load application can be non-uniform, the stress within a biologic structure can vary considerably from region to region. Some regions may bear very little stress while other regions experience very high stresses due to their proximity to a particular loading point or geometric feature. It is important to note that stress is a mathematical quantity that can be calculated, but cannot be measured, felt, or observed. Furthermore, the notion of stress as a mathematical description of mechanical load bearing is distinct from and not synonymous with notions of stress typically used in physiologic or metabolic contexts (*e.g*. ischemic or oxidativestress).

***Strain*** is a measure of the local deformation in a material or tissue induced by an applied stress, and is usually expressed as the percentage change in length of the original geometry (*e.g*. a wire that was originally 10 mm long that has been stretched an additional 1 mm, exhibits 10% strain). Like stress, strain may also be decomposed into normal (tensile or compressive) and shear (distortional) components (Figure 3). It is important to recognize that strain, unlike stress, may be observed and measured. It is also important to appreciate the distinction between the deformation of a structure and strain within its constituent parts. While a structure may exhibit

NIH-PA Author Manuscript

NIH-PA Author Manuscript

NIH-PA Author Manuscript

an overall, global deformation in response to an applied load, the localized relative displacement described by the strain provides a measurable indicator of the level of micro-deformation (stretch, compression, or shearing) experienced by the tissue. This distinction has important consequences in biomechanics at all levels, because it is strain, not stress that causes damage to tissues[11]. Furthermore, mechanosensation by cells is likely dependent on the local deformations associated with tissue strain and may play a role in tissue remodeling.

The ***material properties*** of a tissue describe its ability to resist deformation under applied load and therefore relate *stress* to *strain* (*i.e.* load to deformation). Material properties can be thought of as the stiffness or compliance of a particular tissue or material that is intrinsic to the material itself. Hence, a stiff tissue such as sclera can have high stress, but low strain, while an equal volume of compliant tissue like retina might have high strain even at low levels of stress. Material properties are generally determined through rigorous experimental testing of the material in tension, compression, and shear.

Material properties are often described in terms of their material symmetry (isotropic or anisotropic), the nature of the relationship between load and deformation (linear or nonlinear), and the time-dependence of their response to loading (elastic or viscoelastic). Isotropic materials exhibit identical resistance to load in all directions while anisotropic materials can exhibit higher or lower stiffness properties along different directions. For instance, concrete may be isotropic by itself, but the introduction of rebar during fabrication would produce an anisotropic material with higher resistance to tension along the direction of the rebar. The load-deformation, or stress-strain relationship that characterizes a material can also be described in terms of whether it is linear or nonlinear. In linear materials, stress is directly proportional to strain, by a constant factor known as the Young's modulus. Nonlinear materials, on the other hand, have a non-constant proportionality between stress and strain, and hence don't have a unique or constant Young's modulus. Figure 4 illustrates the behavior of a nonlinear anisotropic material. Finally, the response of some materials is time-dependent. Viscoelastic materials, for instance, when loaded quickly exhibit higher resistance than when loaded slowly (similar to a hydraulic shock absorber). They also exhibit creep under constant load, or stress-relaxation under constant displacement. In contrast, the stiffness of elastic materials is not dependent on the rate of load application and these materials do not exhibit creep or stress relaxation phenomena.

The simplest material property description is that of an isotropic, linearly elastic material (*e.g.*, steel). Biologic soft tissues (*e.g.*, sclera or tendon), are usually nonlinear, anisotropic, viscoelastic materials and so exhibit increased resistance to strain at higher load levels, are stiffer when loaded in a particular direction, and respond to load in a rate- and time-dependent manner. Characterization of the material properties of biologic soft tissues is a formidable undertaking and requires extensive experimental effort. Once established, material descriptions for tissues may be used in conjunction with descriptions of geometry and loading conditions to model the stress and strain fields borne throughout a structure.

Another useful concept in biomechanics is ***structural stiffness***, which incorporates both the material properties and geometry of a complex load bearing structure into a composite measure of the structure's resistance to deformation. In the eye, both the geometry and material properties of the sclera and lamina cribrosa contribute to the structural stiffness of the ONH and peripapillary sclera, and hence determine their ability to withstand strain when exposed to IOP. As such, individual ONH biomechanics is governed by the geometry (size and shape of the scleral canal, scleral thickness, regional laminar density and beam orientation) and the material properties (stiffness) of the lamina cribrosa and sclera. Hence, two eyes exposed to identical IOPs may exhibit very different strain fields due to differences in their structural stiffness (Figure 5).

NIH-PA Author Manuscript

NIH-PA Author Manuscript

NIH-PA Author Manuscript

***Mechanical yield*** occurs when a material is strained beyond its elastic limit, and is therefore unable to return to its undeformed shape. A material or tissue that has yielded in response to high strains is permanently damaged and deformed and is usually less resistant to further loading (hypercompliance). ***Mechanical failure*** occurs at even higher strain, typically follows yield, and generally manifests in soft tissues as catastrophic rupture or pulling apart. For any individual ONH there will likely be an IOP that induces widespread yield in the laminar beams, but does not result in visible failure of individual trabeculae. At even higher IOPs, some catastrophic failure of individual laminar beams will be evident, while a new population of beams may now demonstrate yield. Yield and failure are short-term mechanical processes that likely induce a long-term cellular remodeling response that serves to restructure the ONH to alter its future load bearing capacity. Early connective tissue damage likely leads to tissue remodeling that may make the remaining connective tissues and axons more susceptible to additional damage at all levels of IOP. This notion is of central importance in the controversies regarding the importance of treating ocular hypertensive patients prior to the onset of clinically detectable glaucomatous damage.

## B. Overview of the Mechanical Environment of the ONH and Peripapillary Sclera

From an engineering perspective, the eye is a vessel with inflow and outflow facilities that regulate its internal pressure. IOP imposes a pressure load normal to the inner surface of the eye wall, generating an in-wall circumferential stress known as the hoop stress (Figure 6). This IOP-generated stress is primarily borne by the stiff, collagenous sclera, while the more compliant retina and nerve fiber tissues bear little of the in-wall stress load and are therefore exposed primarily to the compressive stress of IOP. IOP is borne in the ONH by the fenestrated connective tissues of the lamina cribrosa, which span the scleral canal opening and tether into the stiff outer ring of circumferential collagen and elastin fibers in the peripapillary sclera (like the fabric in a trampoline tethering to the frame with springs). While Laplace's Law[10] is useful to describe the pressure-deformation relationship in a spherical vessel of uniform thickness, it is wholly inadequate for describing the eye's response to variations in IOP (Figures 5 and 7). It is important to note that the in-wall hoop stress dominates laminar biomechanics, and the hoop stress is approximately 15 times greater than the stress generated by the translaminar pressure gradient (Figure 7).

There are several characteristics of the ocular load-bearing tissues that complicate the study of the mechanical environment to which the ONH and its resident cell populations are exposed. First, the three-dimensional connective tissue geometry of the eye is complex and difficult to measure. For instance, the thickness of monkey sclera can vary as much as 4-fold from the equator to the peripapillary region[12, 13] and the 3D morphology of lamina cribrosa is more regionally complex and individualized than is generally appreciated[14-17]. Second, the cornea, sclera and lamina cribrosa have extremely complex ECM microstructures with highly anisotropic collagen and elastin fibril orientations. As a result, the *experimental* characterization and *theoretical/mathematical* description of their constituent material properties are complex and difficult to obtain. Third, the cells that maintain the ocular connective tissues are biologically active. As such, the geometry and material properties of the sclera and lamina cribrosa change in response to both physiologic (age) and pathologic (both IOP-related and non-IOP-related) factors. Fourth, the eye is exposed to ever changing loading conditions because IOP undergoes acute, short-term and long-term fluctuations ranging from blinks and eye rubs to circadian rhythms.

Finally, IOP-related stress generates strain patterns in the ONH and peripapillary sclera that are not only dependent on differing connective tissue geometries and material properties but are also influenced by complex loading conditions. The important factors contributing to this biomechanical component include the alignment and density of collagen fibrils in each tissue

NIH-PA Author Manuscript

NIH-PA Author Manuscript

NIH-PA Author Manuscript

(stiffness and anisotropy), the rate of change in IOP (via tissue viscoelasticity) and the level of IOP-related strain at the time of altered loading (via tissue nonlinearity). In broad terms, the ONH connective tissues should be stiffer when there is already considerable strain present and/or if the IOP load is applied quickly. Conversely, the ONH should be more compliant in response to slow changes in IOP and/or at low levels of strain.

### C. Mechanical Response of the ONH to Acutely Elevated IOP

It is important to note that the ONH responds to IOP elevations as a structural system, so the acute mechanical response of the lamina cribrosa is confounded with the responses of the peripapillary sclera, prelaminar neural tissues, and retrolaminar optic nerve. Because the lamina lies buried underneath the prelaminar neural tissues and the acute structural responses of these two tissues to acute IOP elevations are quite different, it is likely that acute laminar deformation cannot be directly measured from imaging the surface topography of the ONH[18]. A final confounding effect is the cerebrospinal fluid pressure, which along with IOP, determines the translaminar pressure gradient that must be borne by the lamina cribrosa (Figure 7).

Intuitively, it may seem that for a given acute increase in IOP, the lamina cribrosa should deform posteriorly and there have been several experimental studies designed to measure acute IOP-related laminar deformation. Yan and co-workers found that increasing IOP from 5 to 50 mm Hg for 24 hours produced an average posterior deformation of the central lamina of 79 μm in human donor eyes[19]. Levy and Crapps reported a 12 μm average posterior movement of the central lamina with acute IOP elevations from 10 to 25 mm Hg for shorter time periods in human eyes[20].

More recently, Bellezza and colleagues reported a small but significant posterior laminar deformation of 10 to 23 μm (95% confidence interval (CI)) in a histologic evaluation of monkey eyes perfusion fixed with one eye at 10 mm Hg and the contralateral eye at 30 or 45 mm Hg for 15 minutes prior to death[21]. However, these deformations, while statistically significant, did not substantially exceed the 95% CI for intra-animal physiologic differences (1 to 17 μm) between normal eyes bilaterally immersion fixed at an IOP of 0 mm Hg.

The previous studies were performed using two-dimensional (2D), measurements of laminar compliance within actual histologic sections. Angled sectioning, section warping, and the lack of a stable measurement reference plane can influence the accuracy of this technique. To overcome these problems, Downs, Yang, and co-workers developed a technique for 3D delineation and measurement of ONH structures within high resolution, digital 3D reconstructions[22-25]. While our initial reports have concentrated on monkeys with early experimental glaucoma in one eye, preliminary data from a larger group of bilaterally normal monkeys perfusion fixed with both eyes at an IOP of 10 mm Hg ($n$=5), one eye at 10 mm Hg, the other at 30 mm Hg ($n$=3), and one eye at 10 mm Hg, the other at 45 mm Hg ($n$=3) suggest that while acute IOP elevation causes expansion of the scleral canal, in most monkey eyes there is no net posterior laminar deformation from the plane of the sclera. Thus, our current understanding of the aggregate response of the young adult monkey ONH to acute IOP elevation is that expansion of the scleral canal tightens the lamina within the plane of the sclera, making it more resistant to posterior deformation out of that plane (Figure 8). These data are preliminary and our interpretation may change with further study.

It is important to note that the lack of laminar deformation in these eyes does not mean that the lamina is not strained. In this scenario, the expansion of the canal stretches the lamina cribrosa within the plane of the sclera generating substantial strain within the laminar beams. Estimation of laminar beam strain within these same 3D reconstructions is one of the outputs of finite

NIH-PA Author Manuscript

NIH-PA Author Manuscript

NIH-PA Author Manuscript

element modeling - an engineering technique that is currently being applied to the ONH by our[17, 26] and other[27, 28] laboratories.

### D. The Contribution of the Sclera to ONH Biomechanics

The data described above, as well as the computational models reported to date[17, 26-28] suggest that the sclera plays an important role in ONH biomechanics. The peripapillary sclera provides the boundary conditions for the ONH. By this we mean that the peripapillary sclera is the tissue through which load and deformation are transmitted to the ONH, and that the structural stiffness of the peripapillary sclera, therefore, influences how the lamina deforms (Figures 5, 7, 8). This can be understood from the discussion above in which a compliant sclera allows the scleral canal to expand following an acute IOP elevation, tightening the laminar beams within the canal and thereby increasing laminar resistance to posterior deformation. In contrast, a rigid sclera allows less expansion of the canal or none at all, forcing the structural stiffness of the lamina alone to bear the IOP-related stress. Hence, as is evidenced by the difficulties in measuring true IOP through the cornea[29, 30],characterization of both components of scleral structural stiffness (geometry and material properties) is essential to understanding the effects of IOP on the ONH.

### F. Other IOP-related Changes in the ONH

ONH, retinal, and choroidal blood flow are all affected in different ways by acute[31-35] IOP elevations. Previous studies using microspheres[32, 33] have suggested that volume flow within the prelaminar and anterior laminar capillary beds is preferentially diminished once ocular perfusion pressure (defined as the systolic arterial blood pressure plus 1/3 of the difference between systolic and diastolic pressures minus IOP) is less than 30 mm Hg.

While a direct link to mechanical strain has not been established, axonal transport is compromised in the lamina cribrosa at physiologic levels of IOP[36, 37] and is further impaired following acute IOP elevations[6, 7, 37, 38]. Several hypotheses regarding this behavior emerge when considering ONH biomechanics. First, as the pores in the lamina cribrosa change conformation due to IOP-related mechanical strain, the path of the axons through those pores may be disrupted thereby directly impeding axoplasmic transport. Second, it may be that the IOP-related reduction in blood flow in the laminar region impairs the mitochondrial metabolism that drives axoplasmic transport. Finally, axoplasmic transport could be sensitive to the magnitude of the translaminar pressure gradient, and as that hydrostatic pressure gradient gets larger with increasing IOP (or lower cerebrospinal fluid pressure), the mechanisms driving that transport are unable to overcome the resistance of the pressure gradient (Figure 7). Recent histologic work in the monkey model of glaucoma has show that the prelaminar neural tissues are significantly thickened at the earliest detectable stage of glaucoma (Figure 9)[25]. Reversible axonal transport blockade followed by secondary axonal swelling may importantly contribute to this phenomenon.

In summary, while connective tissue dynamics should directly and indirectly influence astrocyte and glial metabolism as well as axonal transport, glaucomatous damage within the ONH may not necessarily occur at locations with the highest levels of IOP-related connective tissue strain. Axoplasmic transport disruption and eventual axonal damage may first occur at those locations where the translaminar tissue pressure gradient is greatest[18, 39] and/or where the axons, blood supply, astrocytes and glia are most vulnerable to IOP-related insult. Further studies are necessary to elucidate the link(s) between IOP, mechanical strain, blood flow, astrocyte and glial cell homeostasis, and axoplasmic transport in the ONH, in both the physiologic and diseased states.

NIH-PA Author Manuscript

NIH-PA Author Manuscript

NIH-PA Author Manuscript

# IV. Future Directions

## A. Clinical Implications

There are currently no science-based tools to predict at what level of IOP an individual ONH will be damaged. Finite element modeling is a computational tool for predicting how a biological tissue of complicated geometry and material properties will behave under varying levels of load. The goal of basic research finite element modeling in monkey and human cadaver eyes is to learn what aspects of ONH neural, vascular and connective tissue architecture are most important to the ability of a given ONH to maintain structural integrity, nutritional homeostasis and axoplasmic transport at physiologic and non-physiologic levels of IOP. In the future, clinical imaging of the ONH will seek to capture the architecture of these structures to allow clinically derived biomechanical models of the ONHs of individual patients to make predictions regarding physiologic and pathophysiologic levels of IOP. Eventually knowing the relationship between IOP, mechanical strain, systemic blood pressure, and some measure of astrocyte and axonal homeostasis such as cellular or mitochondrial oxygen saturation or oxidation[40-44] may drive the clinical assessment of safe target IOP.

In selected patients, constant clinical measurement of IOP magnitude and fluctuation through telemetric monitoring will enable the first accurate characterization of IOP-related risk and therefore better-controlled studies of ONH directed neuroprotection. Finally, finite element model-driven targets for sub-surface ONH imaging will allow early detection of lamina cribrosa deformation and thickening (Figures 9 and 10). Once clinically detectable, early stabilization and possibly reversal of these laminar and prelaminar changes (Figure 10) will become a new end point for target IOP lowering in high risk ocular hypertensive and all progressing eyes.

## B. Basic Research Directions

From an engineering standpoint, large challenges remain to achieve basic and clinical knowledge regarding: 1) the mechanisms and distributions of IOP-related yield and failure in the laminar beams and peripapillary sclera; 2) the mechanobiology of the astrocytes, scleral fibroblasts, and lamina cribrosa and glial cells; 3) the mechanobiology of axoplasmic flow within the lamina cribrosa; 4) the fluid dynamics governing the volume flow of blood within the laminar capillaries and scleral and laminar branches of the posterior ciliary arteries; and 5) nutrient diffusion to the astrocytes in young and aged eyes. However, if successful, knowledge gained from these studies will importantly contribute to new therapeutic interventions aimed at the ONH and peripapillary sclera of glaucomatous eyes.

# References

1. Yucel YH, Zhang Q, Gupta N, Kaufman PL, Weinreb RN. Loss of neurons in magnocellular and parvocellular layers of the lateral geniculate nucleus in glaucoma. Arch Ophthalmol 2000;118:378–384. [PubMed: 10721961]
2. Gupta N, Yucel Y. Glaucoma and the Brain. Journal of Glaucoma 2001;10:S28–S29. [PubMed: 11890268]
3. Yucel YH, Zhang Q, Weinreb RN, Kaufman PL, Gupta N. Atrophy of relay neurons in magno- and parvocellular layers in the lateral geniculate nucleus in experimental glaucoma. Invest Ophthalmol Vis Sci 2001;42:3216–3222. [PubMed: 11726625]
4. Yucel YH, Zhang Q, Weinreb RN, Kaufman PL, Gupta N. Effects of retinal ganglion cell loss on magno-, parvo-, koniocellular pathways in the lateral geniculate nucleus and visual cortex in glaucoma. Prog Retin Eye Res 2003;22:465–481. [PubMed: 12742392]
5. Anderson DR, Hendrickson A. Effect of intraocular pressure on rapid axoplasmic transport in monkey optic nerve. invest Ophthalmol Vis Sci 1974;13:771–783.

NIH-PA Author Manuscript

NIH-PA Author Manuscript

NIH-PA Author Manuscript


6. Minckler DS, Bunt AH, Johanson GW. Orthograde and retrograde axoplasmic transport during acute ocular hypertension in the monkey. Invest Ophthalmol Vis Sci 1977;16:426–441. [PubMed: 67096]
7. Quigley H, Anderson DR. The dynamics and location of axonal transport blockade by acute intraocular pressure elevation in primate optic nerve. Invest Ophthalmol Vis Sci 1976;15:606–616.
8. Burgoyne CF, Downs JC, Bellezza AJ, Suh JK, Hart RT. The optic nerve head as a biomechanical structure: a new paradigm for understanding the role of IOP-related stress and strain in the pathophysiology of glaucomatous optic nerve head damage. Prog Retin Eye Res 2005;24:39–73. [PubMed: 15555526]
9. Ethier, CR.; Simmons, CA. Introductory Biomechanics: From Cells to Organisms. Vol. 1 edn.. Cambridge University Press; New York: 2007.
10. Timoshenko, SP. Theory of Elasticity. Vol. Third edn.. McGraw-Hill Book Co; New York: 1970.
11. Sigal IA, Flanagan JG, Tertinegg I, Ethier CR. Predicted extension, compression and shearing of optic nerve head tissues. Exp Eye Res 2007;85:312–322. [PubMed: 17624325]
12. Downs JC, Ensor ME, Bellezza AJ, et al. Posterior Scleral Thickness in Perfusion-Fixed Normal and Early-Glaucoma Monkey Eyes. Invest Ophthalmol Vis Sci 2001;42:3202–3208. [PubMed: 11726623]
13. Downs JC, Blidner RA, Bellezza AJ, et al. Peripapillary scleral thickness in perfusion-fixed normal monkey eyes. Invest Ophthalmol Vis Sci 2002;43:2229–2235. [PubMed: 12091421]
14. Dandona L, Quigley HA, Brown AE, Enger C. Quantitative regional structure of the normal human lamina cribrosa. A racial comparison. Arch Ophthalmol 1990;108:393–398. [PubMed: 2310342]
15. Quigley HA, Addicks EM. Regional differences in the structure of the lamina cribrosa and their relation to glaucomatous optic nerve damage. Arch Ophthalmol 1981;99:137–143. [PubMed: 7458737]
16. Radius RL. Regional specificity in anatomy at the lamina cribrosa. Arch Ophthalmol 1981;99:478–480. [PubMed: 7213169]
17. Roberts, MD.; Hart, RT.; Liang, Y., et al. ASME Summer Bioengineering Conference. American Society of Mechanical Engineers; Keystone, CO: 2007. Continuum-level finite element modeling of the optic nerve head using a fabric tensor based description of the lamina cribrosa..
18. Morgan WH, Chauhan BC, Yu D-Y, et al. Optic Disc Movement with Variations in Intraocular and Cerebrospinal Fluid Pressure. Invest Ophthalmol Vis Sci 2002;43:3236–3242. [PubMed: 12356830]
19. Yan DB, Coloma FM, Metheetrairut A, et al. Deformation of the lamina cribrosa by elevated intraocular pressure. Br J Ophthalmol 1994;78:643–648. [PubMed: 7918293]
20. Crapps EE, Levy NS. Displacement of the lamina scleralis with pressure elevation. Invest Ophthalmol Vis Sci 1981;20:82.
21. Bellezza AJ, Rintalan CJ, Thompson HW, et al. Deformation of the lamina cribrosa and anterior scleral canal wall in early experimental glaucoma. Invest Ophthalmol Vis Sci 2003;44:623–637. [PubMed: 12556392]
22. Burgoyne CF, Downs JC, Bellezza AJ, Hart RT. Three-dimensional reconstruction of normal and early glaucoma monkey optic nerve head connective tissues. Invest Ophthalmol Vis Sci 2004;45:4388–4399. [PubMed: 15557447]
23. Downs JC, Yang H, Girkin C, et al. Three Dimensional Histomorphometry of the Normal and Early Glaucomatous Monkey Optic Nerve Head: Neural Canal and Subarachnoid Space Architecture. Invest Ophthalmol Vis Sci 2007;48:3195–3208. [PubMed: 17591889]
24. Yang H, Downs JC, Girkin C, et al. 3-D Histomorphometry of the Normal and Early Glaucomatous Monkey Optic Nerve Head: Lamina Cribrosa and Peripapillary Scleral Position and Thickness. Invest Ophthalmol Vis Sci. 2007In Press
25. Yang H, Downs JC, Bellezza AJ, Thompson H, Burgoyne CF. 3-D Histomorphometry of the Normal and Early Glaucomatous Monkey Optic Nerve Head: Prelaminar Neural Tissues and Cupping. Invest Ophthalmol Vis Sci. 2007In Press
26. Downs, JC.; Roberts, MD.; Burgoyne, CF.; Hart, RT. Finite Element Modeling of the Lamina Cribrosa Microarchitecture in the Normal and Early Glaucoma Monkey Optic Nerve Head.. ASME Summer Bioengineering Conference.; Keystone, CO: American Society of Mechanical Engineers. 2007.
27. Sigal IA, Flanagan JG, Ethier CR. Factors influencing optic nerve head biomechanics. Invest Ophthalmol Vis Sci 2005;46:4189–4199. [PubMed: 16249498]

NIH-PA Author Manuscript

NIH-PA Author Manuscript

NIH-PA Author Manuscript


28. Sigal IA, Flanagan JG, Tertinegg I, Ethier CR. Finite element modeling of optic nerve head biomechanics. Invest Ophthalmol Vis Sci 2004;45:4378–4387. [PubMed: 15557446]
29. Liu J, Roberts CJ. Influence of corneal biomechanical properties on intraocular pressure measurement: quantitative analysis. J Cataract Refract Surg 2005;31:146–155. [PubMed: 15721707]
30. Brandt JD, Beiser JA, Kass MA, Gordon MO. Central corneal thickness in the Ocular Hypertension Treatment Study (OHTS). Ophthalmology 2001;108:1779–1788. [PubMed: 11581049]
31. Alm A, Bill A. The oxygen supply to the retina. II. Effects of high intraocular pressure and of increased arterial carbon dioxide tension on uveal and retinal blood flow in cats. A study with radioactively labelled microspheres including flow determinations in brain and some other tissues. Acta Physiol Scand 1972;84:306–319. [PubMed: 4553229]
32. Geijer C, Bill A. Effects of raised intraocular pressure on retinal, prelaminar, laminar, and retrolaminar optic nerve blood flow in monkeys. Invest Ophthalmol Vis Sci 1979;18:1030–1042. [PubMed: 90027]
33. Alm A, Bill A. Ocular and optic nerve blood flow at normal and increased intraocular pressures in monkeys (Macaca irus): a study with radioactively labelled microspheres including flow determinations in brain and some other tissues. Exp Eye Res 1973;15:15–29. [PubMed: 4630581]
34. Alm A, Bill A. Blood flow and oxygen extraction in the cat uvea at normal and high intraocular pressures. Acta Physiol Scand 1970;80:19–28. [PubMed: 5475327]
35. Sossi N, Anderson DR. Effect of elevated intraocular pressure on blood flow. Occurrence in cat optic nerve head studied with iodoantipyrine I 125. Arch Ophthalmol 1983;101:98–101. [PubMed: 6849662]
36. Ernest JT, Potts AM. Pathophysiology of the distal portion of the optic nerve. I. Tissue pressure relationships. Am J Ophthalmol 1968;66:373–380. [PubMed: 5676350]
37. Minckler D. Correlations between anatomic features and axonal transport in primate optic nerve head. Tr Am Ophth Soc vol LXXXIV 1986:429–451.
38. Quigley HA, Anderson DR. Distribution of axonal transport blockade by acute intraocular pressure elevation in the primate optic nerve head. Invest Ophthalmol Vis Sci 1977;16:640–644. [PubMed: 68942]
39. Jonas JB, Berenshtein E, Holbach L. Lamina cribrosa thickness and spatial relationships between intraocular space and cerebrospinal fluid space in highly myopic eyes. Invest Ophthalmol Vis Sci 2004;45:2660–2665. [PubMed: 15277489]
40. Bristow EA, Griffiths PG, Andrews RM, Johnson MA, Turnbull DM. The distribution of mitochondrial activity in relation to optic nerve structure. Arch Ophthalmol 2002;120:791–796. [PubMed: 12049585]
41. Tezel G, Yang X, Luo C, et al. Mechanisms of Immune System Activation in Glaucoma: Oxidative Stress-Stimulated Antigen Presentation by the Retina and Optic Nerve Head Glia. Invest Ophthalmol Vis Sci 2007;48:705–714. [PubMed: 17251469]
42. Tezel G, Luo C, Yang X. Accelerated Aging in Glaucoma: Immunohistochemical Assessment of Advanced Glycation End Products in the Human Retina and Optic Nerve Head. Invest Ophthalmol Vis Sci 2007;48:1201–1211. [PubMed: 17325164]
43. Barron MJ, Griffiths P, Turnbull DM, Bates D, Nichols P. The distributions of mitochondria and sodium channels reflect the specific energy requirements and conduction properties of the human optic nerve head. Br J Ophthalmol 2004;88:286–290. [PubMed: 14736793]
44. Abu-Amero KK, Morales J, Bosley TM. Mitochondrial abnormalities in patients with primary open-angle glaucoma. Invest Ophthalmol Vis Sci 2006;47:2533–2541. [PubMed: 16723467]
45. Anderson DR. Ultrastructure of human and monkey lamina cribrosa and optic nerve head. Arch Ophthalmol 1969;82:800–814. [PubMed: 4982225]
46. Quigley HA, Brown AE, Morrison JD, Drance SM. The size and shape of the optic disc in normal human eyes. Arch Ophthalmol 1990;108:51–57. [PubMed: 2297333]
47. Cioffi, GA.; Van Buskirk, EM. Vasculature of the anterior optic nerve and peripapillary choroid.. In: Ritch, R.; Shields, MB.; Krupin, T., editors. The Glaucomas. Basic Sciences; Mosby, St. Louis: 1996. p. 177-197.

NIH-PA Author Manuscript

NIH-PA Author Manuscript

NIH-PA Author Manuscript

48. Quigley, HA. Overview and introduction to session on connective tissue of the optic nerve in glaucoma.. In: Drance, SM.; Anderson, DR., editors. Optic Nerve in Glaucoma. Kugler Publications; Amsterdam/New York: 1995. p. 15-36.Chapter 2

49. Morrison JC, L'Hernault NL, Jerdan JA, Quigley HA. Ultrastructural location of extracellular matrix components in the optic nerve head. Arch Ophthalmol 1989;107:123–129. [PubMed: 2910271]

NIH-PA Author Manuscript
NIH-PA Author Manuscript
NIH-PA Author Manuscript



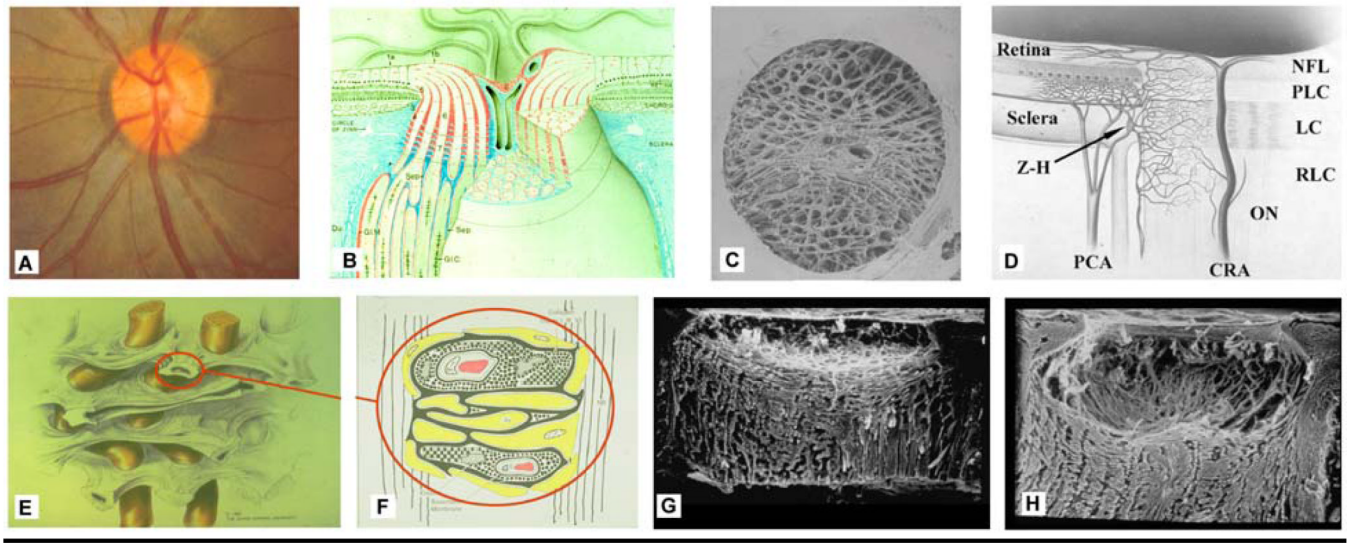


**Figure 1. The optic nerve head (ONH) is a three-dimensional (3D) structure comprised of multiple interactive tissue systems that exist on different scales. This complexity has been a formidable deterrent to characterizing its mechanical environment**

**(A)** While clinicians are familiar with the clinically visible surface of the optic nerve head (referred to as the optic disc), in fact the ONH **(B)** is a dynamic, 3D structure (seen here in an illustrated sectional view) in which the retinal ganglion cell (RGC) axons in bundles (white) surrounded by glial columns (red), pass through the connective tissue beams of the lamina cribrosa (light blue), isolated following trypsin digestion in an scanning electron micrograph (SEM) of the scleral canal in **(C).** The blood supply for the connective tissues of the lamina cribrosa **(D)** derives from the posterior ciliary arteries and the circle of Zinn-Haller (Z-H). **(E-F)** The relationship of the laminar beams to the axon bundles is shown in schematic form in **(E). (F)** Individual beams of the lamina cribrosa are lined by astrocytes. Together they provide structural and metabolic support for the adjacent axon bundles. Within the lamina, the RGC axons have no direct blood supply. Axonal nutrition requires diffusion of nutrients from the laminar capillaries (solid red), across the endothelial and pericyte basement membranes, through the extracellular matrix (ECM) of the laminar beam (stippled), across the basement membranes of the astrocytes (thick black), into the astrocytes (yellow), and across their processes (not shown) to the adjacent axons (vertical lines). Chronic age-related changes in the endothelial cell and astrocyte basement membranes, as well as intraocular pressure (IOP)-induced changes in the laminar ECM and astrocyte basement membranes may diminish nutrient diffusion to the axons in the presence of a stable level of laminar capillary volume flow. In advanced glaucoma, the connective tissues of the normal lamina cribrosa (sagittal view of the center of the ONH; vitreous above, orbital optic nerve below), **G**) remodel and restructure into a cupped and excavated configuration (**H**). (B) Reprinted with permission from Doug Anderson[45]; (C) reprinted with permission from Quigley HA[46]; (D) reprinted with permission from Cioffi GA[47]; (E) reprinted with permission from Quigley HA[48]; (F) reprinted with permission from Morrison JC[49] (G, H) Courtesy of Harry A. Quigley, MD.

NIH-PA Author Manuscript
NIH-PA Author Manuscript
NIH-PA Author Manuscript



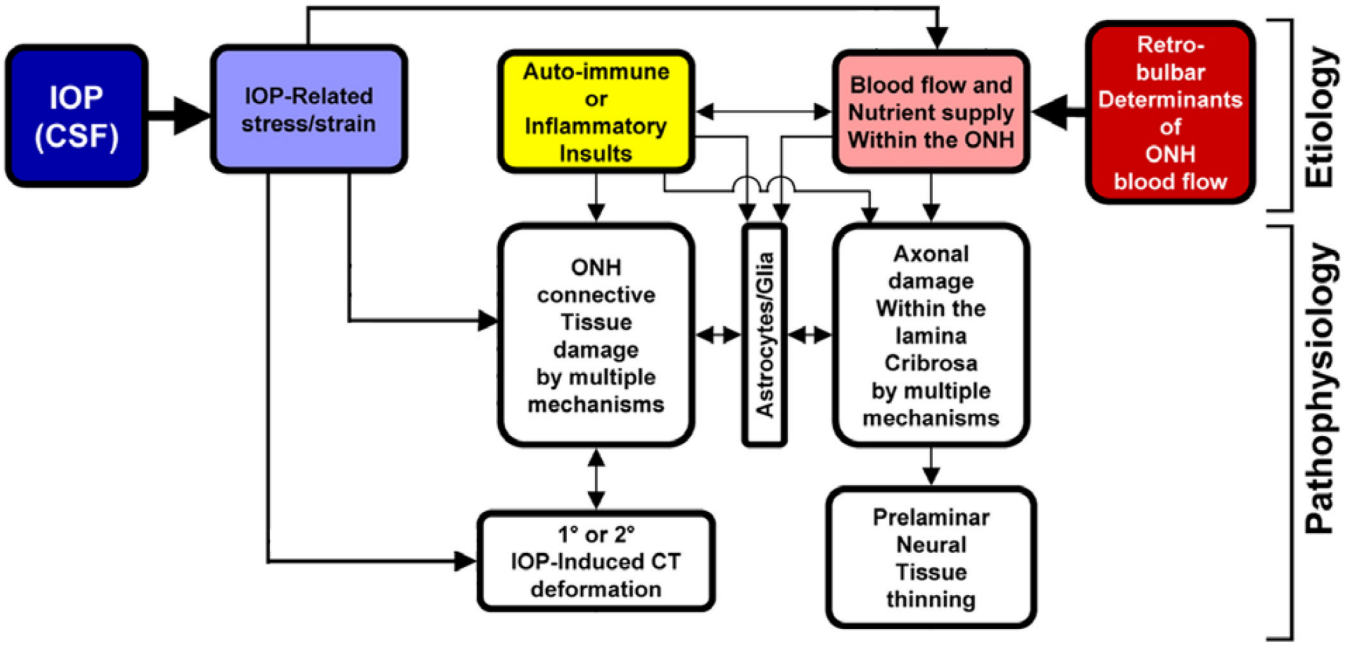


**Figure 2. IOP-related stress and strain are a constant presence within the ONH at all levels of IOP**

In a biomechanical paradigm, IOP-related strain influences the ONH connective tissues and the volume flow of blood (primarily), and the delivery of nutrients (secondarily) through chronic alterations in connective tissue stiffness and diffusion properties (explained in Figure 1). Non-IOP related effects such as auto-immune or inflammatory insults (yellow) and retrobulbar determinants of ocular blood flow (red) can primarily damage the ONH connective tissues and/or axons, leaving them vulnerable to secondary damage by IOP-related mechanisms at normal or elevated levels of IOP. (Based in part on Fig. 5, Journal of Glaucoma Editorial, in press)

NIH-PA Author Manuscript

NIH-PA Author Manuscript

NIH-PA Author Manuscript

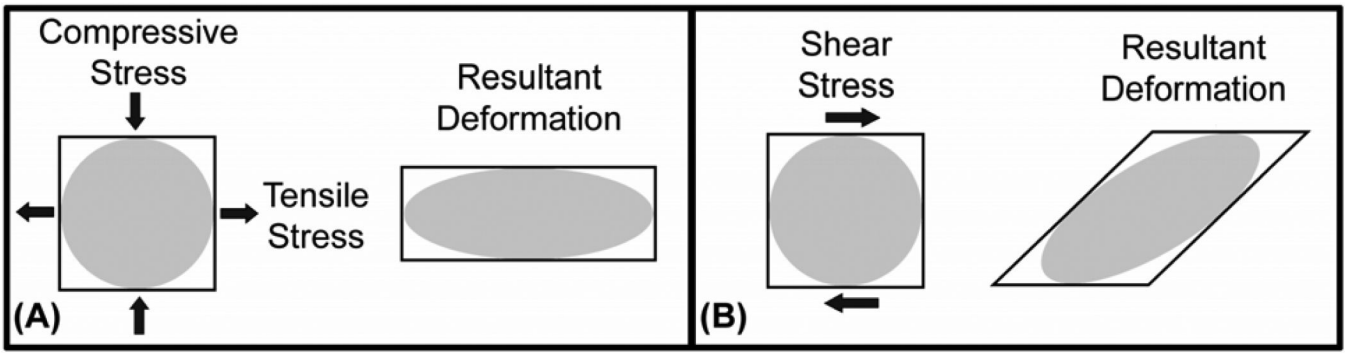


**Figure 3. Normal and shear components of stress and strain**

**(A)** The normal tensile and compressive stresses acting on a small square in the manner shown will act to elongate the region in one direction and compress it in the other. **(B)** The shear stresses acting on a similar region will act to distort the shape of the region.

NIH-PA Author Manuscript

NIH-PA Author Manuscript

NIH-PA Author Manuscript

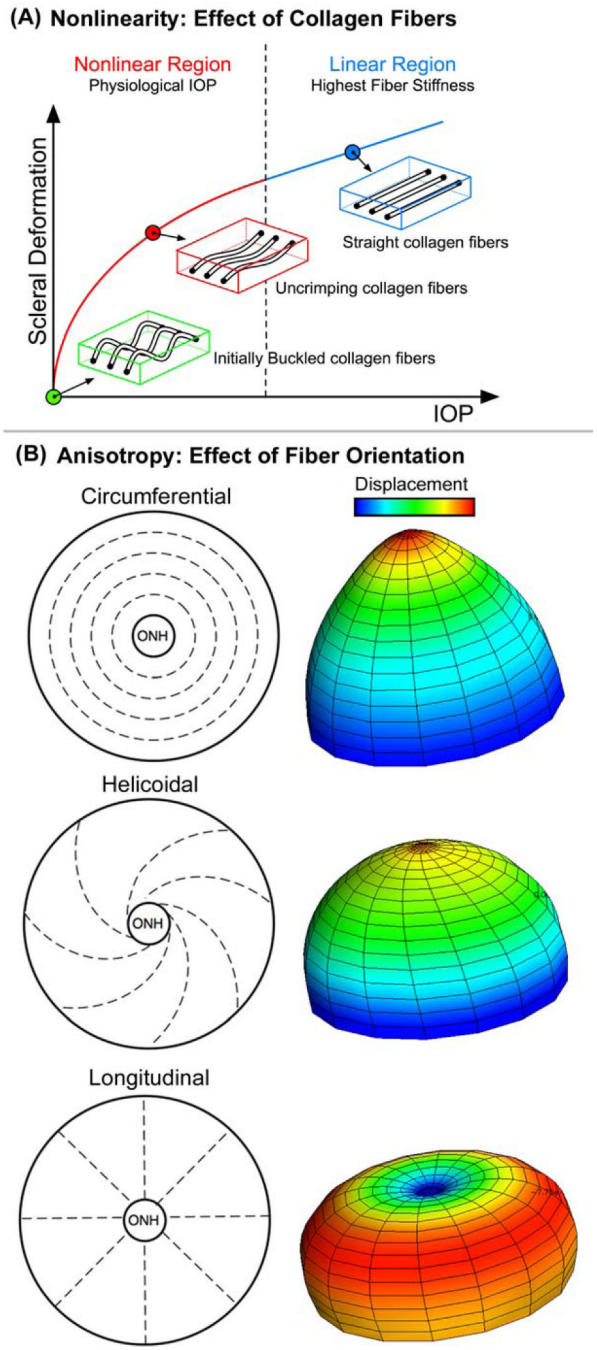


**Figure 4. The material properties of the peripapillary sclera are influenced by nonlinearity and collagen fiber orientation (anisotropy)**

Separate from its thickness, the behavior of the sclera is governed by its material properties, which in turn are influenced by nonlinearity and fiber orientation. **(A)** Nonlinearity is an engineering term for tissues or structures whose material properties are altered by loading. Figure A demonstrates that the sclera becomes stiffer as it is loaded uniaxially (in one direction). In the case of the sclera, this is likely due to the fact collagen fibers embedded within the surrounding ground matrix start out crimped and progressively straighten as the load is increased. This conformational change in the fibrils accounts for the transition from an initially compliant, nonlinear response to a stiffened linear response as IOP increases. **(B)** Apart from

NIH-PA Author Manuscript

NIH-PA Author Manuscript

NIH-PA Author Manuscript

nonlinearity, collagen fiber orientation (anisotropy) within the sclera strongly influences its mechanical behavior. Fiber orientation can be totally random (isotropic - not shown) or have a principal direction (anisotropic – 3 idealized cases shown). Finite element (FE) models of an idealized posterior pole with principal collagen fiber orientation in the circumferential, helicoidal, and longitudinal directions are shown. As the displacement plots show, the underlying fiber orientation can have profound effects on the deformation that occurs for a given IOP. Note that the displacement scale is exaggerated for illustrative purposes. *(Figure courtesy of Michael Girard)*

NIH-PA Author Manuscript
NIH-PA Author Manuscript
NIH-PA Author Manuscript



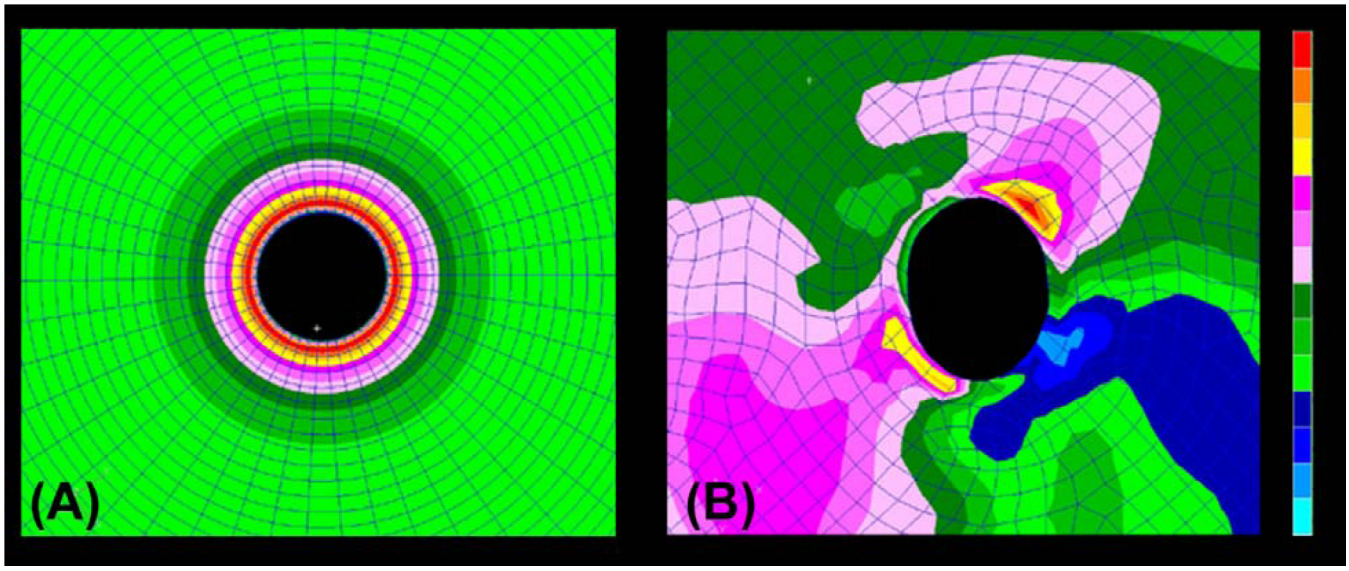


**Figure 5. The thickness of the peripapillary sclera, and the size and shape of the scleral canal influence the magnitude and distribution of IOP-related stress within the peripapillary sclera**

Stress plots within 3D biomechanical models of the posterior sclera and ONH demonstrate that stress concentrates around a defect (scleral canal) in a pressure vessel (eye) and varies according to the geometry of the peripapillary sclera and scleral canal. The idealized model in **(A)** shows the stress concentration around a circular canal in a perfectly spherical pressure vessel with uniform wall thickness (the ONH has been removed from these images for visualization purposes). The model in **(B)** shows the IOP-related stress concentration around an anatomically shaped scleral canal with realistic variation in peripapillary scleral thickness. In this case, the highest stresses (red) occur where the sclera is thinnest and the lowest stresses (blue) occur where the sclera is thickest, and also tend to concentrate around areas of the scleral canal with the smallest radius of curvature. The response of the sclera to this load is determined by its structural stiffness, which is the combination of geometry (how much tissue is bearing the load) and material properties (how rigid or compliant is the tissue).

NIH-PA Author Manuscript

NIH-PA Author Manuscript

NIH-PA Author Manuscript

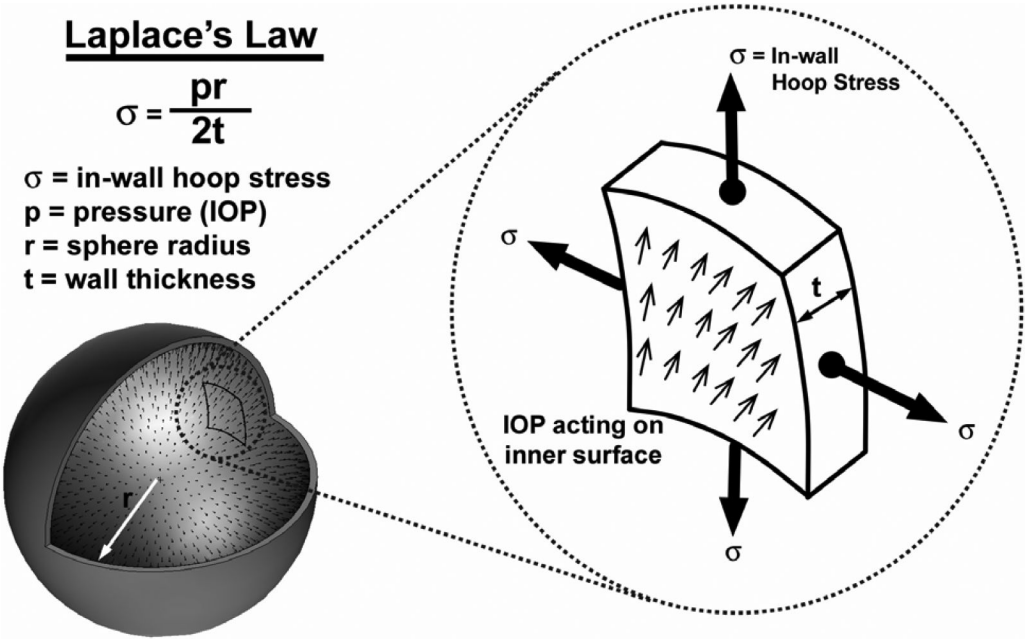


**Figure 6. In-wall stress engendered by IOP loading**

In an idealized spherical shell, the majority of the stress generated by IOP is transferred into a hoop stress borne within the thickness of the wall. Laplace's Law, which relates the in-wall hoop stress to the internal pressure, is only applicable to spherical pressure vessels with isotropic material properties and uniform wall thickness, and can only be used to calculate very rough estimates of hoop stress in actual eyes. In pressure vessel geometries like the eye, with variable wall thickness, aspherical shape, and anisotropic material properties, the hoop stress may vary substantially by location.

NIH-PA Author Manuscript
NIH-PA Author Manuscript
NIH-PA Author Manuscript



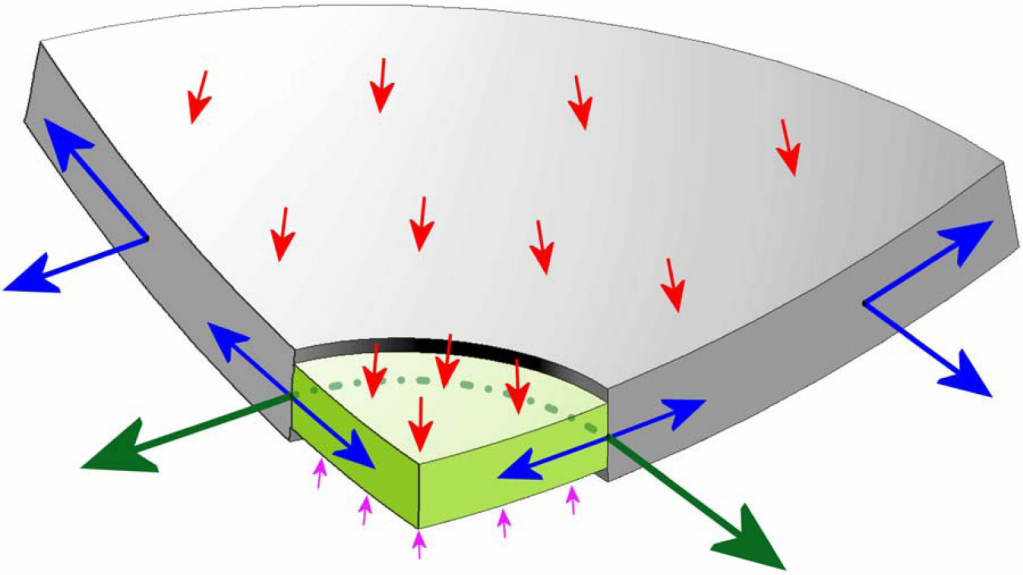

**Figure 7. Stress, relative to IOP (red arrows) in the lamina cribrosa (light green) and peripapillary sclera (grey) engendered by IOP loading**

Cut-away diagram of IOP-induced stress in an idealized spherical scleral shell with a circular scleral canal spanned by a more compliant lamina cribrosa. In this case, the majority of the stress generated by IOP (red arrows) is transferred into a hoop stress borne within the thickness of the sclera and lamina (blue arrows) that is concentrated circumferentially around the scleral canal (green arrows). Note that the difference between IOP (red arrows) and the retrolaminar cerebrospinal fluid pressure (pink arrows) is the translaminar pressure gradient that generates both a net posterior force on the surface of the lamina and a hydrostatic pressure gradient within the neural and connective tissues of the pre-laminar and laminar regions. Most importantly, note that the in-plane hoop stress transferred to the lamina from the sclera is much larger than stress induced by the translaminar pressure gradient.

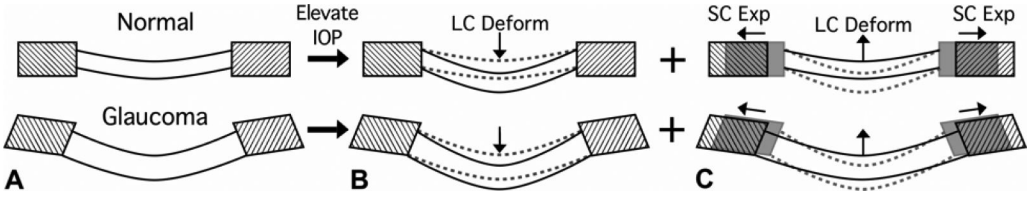


**Figure 8. There are two components of acute IOP-induced ONH deformation in normal and early glaucoma eyes**

**(A)** Sagittal section diagram of the ONH, showing the peripapillary sclera (hatched) and the lamina cribrosa for normal (upper) and early glaucoma (lower) eyes. Note that the early glaucoma eye has undergone permanent changes in ONH geometry including thickening of the lamina, posterior deformation of the lamina and peripapillary sclera, and posterior scleral canal expansion. Upon acute IOP elevation we believe two phenomena occur simultaneously and with interaction: the lamina displaces posteriorly due to the direct action of IOP **(B)**, but much of this posterior laminar displacement is counteracted as the lamina is pulled taut by simultaneous scleral canal expansion **(C)**. It is important to note that even though the net result of these IOP-related deformations is a small amount of posterior displacement of the lamina, substantial levels of IOP-related strain are induced in both the peripapillary sclera and lamina in this scenario.



NIH-PA Author Manuscript
NIH-PA Author Manuscript
NIH-PA Author Manuscript

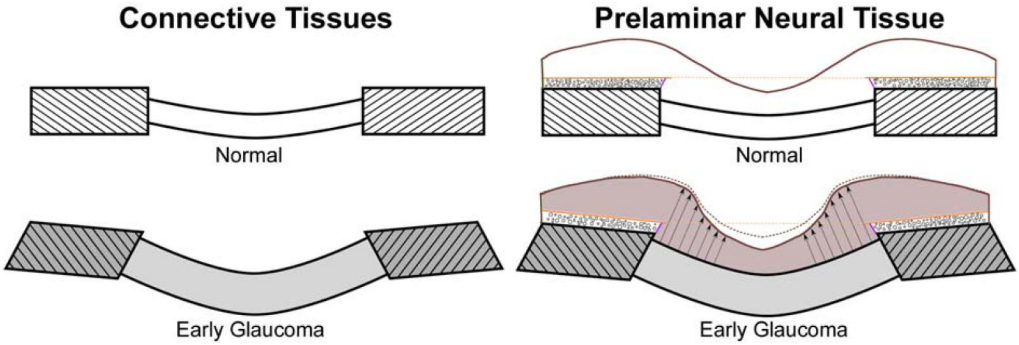


**Figure 9. Remodeling and restructuring of the ONH in early experimental glaucoma[25]**
Sagittal section diagrams of the ONH, showing the peripapillary sclera (hatched) and the lamina cribrosa for normal and early glaucoma eyes. (Left) The early glaucoma eye has undergone permanent changes in ONH geometry including thickening of the lamina, posterior deformation of the lamina and peripapillary sclera, and posterior scleral canal expansion. (Right) Recent work has also shown[25] that although the cup deepens relative to Bruch's membrane opening (dotted orange line) as can be detected by longitudinal confocal scanning laser tomography imaging (solid brown versus dotted brown line) in early glaucoma, the prelaminar neural tissues (grey) are actually thickened (black arrows) rather than thinned. (*Reprinted with permission from Yang, et al.[25]*)



NIH-PA Author Manuscript
NIH-PA Author Manuscript
NIH-PA Author Manuscript

NIH-PA Author Manuscript
NIH-PA Author Manuscript
NIH-PA Author Manuscript



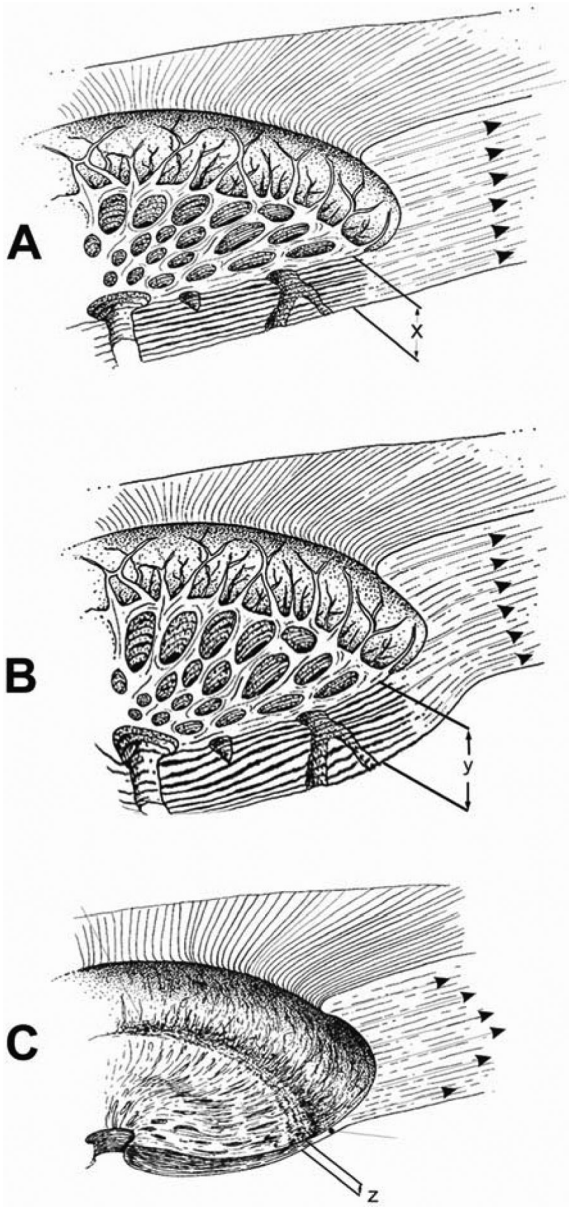


**Figure 10. Progression of connective tissue morphology from normal health to early glaucoma to end-stage glaucoma**

**(A)** Diagram of normal ONH connective tissue showing the thickness of the lamina cribrosa (x) and the in-wall hoop stress generated by IOP in the peripapillary sclera. **(B)** In early experimental glaucoma, our data to date suggests that rather than catastrophic failure of the laminar beams, there is permanent posterior deformation and thickening (y) of the lamina which occurs in the setting of permanent expansion of the posterior scleral canal. These changes indicate that a combination of mechanical yield and subsequent remodeling of the connective tissues occur very early in glaucoma that is not yet accompanied by physical disruption of the beams or frank excavation. **(C)** As the disease progresses to end-stage damage, we believe that the anterior laminar beams eventually fail, the lamina compresses (z) and scars, the laminar insertion into the sclera displaces posteriorly, and the scleral canal enlarges to the typical cupped and excavated morphology. Very little is known about the biomechanics, cellular processes, and remodeling that drives the morphological progression from the earliest

NIH-PA Author Manuscript

NIH-PA Author Manuscript

NIH-PA Author Manuscript

detectable stage of glaucoma to end-stage damage, but it is likely that these processes continue to be driven by the distribution of IOP-related stress and strain within the connective tissues either primarily or through their effects on the capillaries contained within the laminar beams and the adjacent astrocytes. *(Modified from Burgoyne, et al.[8])*